Cell, Vol. 120, 635–647, March 11, 2005, Copyright ©2005 by Elsevier Inc. DOI 10.1016/j.cell.2005.01.014

# *RAS* Is Regulated by the *let-7* MicroRNA Family

**Steven M. Johnson,[1] Helge Grosshans,[1] Jaclyn Shingara,[2] Mike Byrom,[2] Rich Jarvis,[2] Angie Cheng,[2] Emmanuel Labourier,[2] Kristy L. Reinert,[1] David Brown,[2] and Frank J. Slack[1,*]**

[1]Department of Molecular, Cellular and Developmental Biology
Yale University
P.O. Box 208103
New Haven, Connecticut 06520

[2]Ambion, Inc.
2130 Woodward
Austin, Texas 78744

## Summary

**MicroRNAs (miRNAs) are regulatory RNAs found in multicellular eukaryotes, including humans, where they are implicated in cancer. The *let-7* miRNA times seam cell terminal differentiation in *C. elegans*. Here we show that the *let-7* family negatively regulates *let-60/RAS*. Loss of *let-60/RAS* suppresses *let-7*, and the *let-60/RAS* 3′UTR contains multiple *let-7* complementary sites (LCSs), restricting reporter gene expression in a *let-7*-dependent manner. *mir-84,* a *let-7* family member, is largely absent in vulval precursor cell P6.p at the time that *let-60/RAS* specifies the 1° vulval fate in that cell, and *mir-84* overexpression suppresses the multivulva phenotype of activating *let-60/RAS* mutations. The 3′UTRs of the human *RAS* genes contain multiple LCSs, allowing *let-7* to regulate *RAS* expression. *let-7* expression is lower in lung tumors than in normal lung tissue, while RAS protein is significantly higher in lung tumors, providing a possible mechanism for *let-7* in cancer.**

## Introduction

Hundreds of noncoding, regulatory RNAs known as miRNAs (Bartel, 2004), are encoded in animal and plant genomes (Lagos-Quintana et al., 2001; Lau et al., 2001; Lee and Ambros, 2001). miRNAs have emerged as important regulators of development and control processes such as cell fate determination and cell death (Abrahante et al., 2003; Brennecke et al., 2003; Chang et al., 2004; Chen et al., 2004; Johnston and Hobert, 2003; Lee et al., 1993; Lin et al., 2003; Moss et al., 1997; Reinhart et al., 2000; Slack et al., 2000; Wightman et al., 1993). Mounting evidence shows that miRNAs are mutated or poorly expressed in human cancer (Calin et al., 2002; Gauwerky et al., 1989; Lagos-Quintana et al., 2002; McManus, 2003; Michael et al., 2003; Takamizawa et al., 2004; Tam, 2001; Tam et al., 2002), suggesting that miRNAs may act as tumor suppressors or oncogenes. In animals, miRNAs usually control gene expression through complementary elements in the 3′ untranslated regions (UTRs) of their target messenger RNAs (mRNAs) (Lee et al., 1993; Moss et al., 1997; Reinhart et al., 2000; Slack et al., 2000; Vella et al., 2004; Wightman et al., 1993). However, the targets of few mammalian miRNAs are known.

*lethal-7* (*let-7*), a founding member of the miRNA family, is required for timing of cell fate determination in *C. elegans* (Pasquinelli et al., 2000; Reinhart et al., 2000). In wild-type animals, temporal upregulation of *let-7* miRNA in the seam cells (Johnson et al., 2003; Reinhart et al., 2000) is required for their terminal differentiation at the adult stage (Reinhart et al., 2000) when these cells exit the cell cycle, fuse together, and excrete cuticular alae (Sulston and Horvitz, 1977). In *let-7* mutants, seam cells fail to exit the cell cycle and terminally differentiate at the correct time and instead divide (Reinhart et al., 2000), a hallmark of cancer. *let-7* is conserved in many phyla and, like in *C. elegans*, is temporally regulated in *Drosophila* and zebrafish (Pasquinelli et al., 2000). In humans, various *let-7* genes have been reported to map to regions deleted in human cancers (Calin et al., 2004), and *let-7* is poorly expressed in lung cancers (Takamizawa et al., 2004), suggesting that *let-7* miRNAs may be tumor suppressors. In support of this, overexpression of *let-7* inhibited cell growth of a lung cancer cell line in vitro (Takamizawa et al., 2004). However, the mechanism by which *let-7* regulates cell cycle exit in *C. elegans* and human cells is unknown.

*C. elegans let-7*, *mir-48*, *mir-84*, and *mir-241* encode four developmentally regulated miRNAs that comprise the *let-7* family (Lau et al., 2001; Lim et al., 2003; Reinhart et al., 2000). This family displays high sequence identity, with particular conservation at the 5′ end of the mature miRNAs (see Figures S1A and S1B in the Supplemental Data available with this article online). The functions of these family members are unknown. In this paper, we show a role for one of the *C. elegans let-7* family miRNAs, *mir-84*, in vulval development, a model for dissecting RAS/MAP kinase signaling (Wang and Sternberg, 2001). We also show that *C. elegans let-60/RAS* is regulated by members of the *let-7* family. *let-7* and *mir-84* are complementary to multiple sites in the 3′UTR of *let-60/RAS. let-7* and *mir-84* are expressed in a reciprocal manner to *let-60/RAS* in the hypodermis and the vulva, respectively. *let-7* and *mir-84* genetically interact with *let-60/RAS*, consistent with negative regulation of *RAS* expression by *let-7* and *mir-84*. Our results also demonstrate that miRNAs regulate human *RAS*, a critical oncogene. We find that all three human *RAS* genes have *let-7* complementary sites in their 3′UTRs that subject the oncogenes to *let-7* miRNA-mediated regulation in cell culture. Lung tumor tissues display significantly reduced levels of *let-7* and significantly increased levels of RAS protein relative to normal lung tissue, suggesting *let-7* regulation of RAS as a mechanism for *let-7* in lung oncogenesis.

*Correspondence: frank.slack@yale.edu

## Results and Discussion

### *let-60/RAS* as a Target of the *let-7* miRNA in *C. elegans*

The *let-7* miRNA is temporally expressed in *C. elegans* (Johnson et al., 2003; Pasquinelli et al., 2000; Reinhart et al., 2000) where it downregulates at least two target genes, *lin-41* (Slack et al., 2000) and *hbl-1* (Abrahante et al., 2003; Lin et al., 2003), mutations in which lead to precocious terminal differentiation of seam cells. To better understand the role of *let-7* in *C. elegans* seam cell differentiation and its potential role in humans, we sought to identify additional targets of *let-7*. We performed a computational screen for *C. elegans* genes with *let-7* family complementary sites (LCS) in their 3′UTR (Grosshans et al., 2005). One of the top-scoring genes was *let-60*, encoding the *C. elegans* ortholog of the human oncogene *RAS*. We identified eight LCSs in the 3′UTR of *let-60* with features resembling validated LCSs (Lin et al., 2003; Reinhart et al., 2000; Slack et al., 2000; Vella et al., 2004; Figure 1A). Many of the identified sites were found in the 3′UTR of *let-60* from the closely related nematode *C. briggsae* (Stein et al., 2003; Figures 1A, S2A, and S2B), suggesting that they are likely to be biologically significant. An additional three sites were found in the *let-60/RAS* coding sequence as well as 10 other nonconforming 3′UTR sites that may also bind to *let-7* family miRNAs (Figure S2A).

*let-7(n2853ts)* loss-of-function (lf) mutants express reduced *let-7* miRNA and die by bursting at the vulva at the nonpermissive temperature (Reinhart et al., 2000; Slack et al., 2000). Lf mutations in two previously identified targets of *let-7*, *lin-41*, and *hbl-1* have the property of partially suppressing the *let-7* lethal phenotype (Abrahante et al., 2003; Lin et al., 2003; Reinhart et al., 2000; Slack et al., 2000). We found that postembryonic reduction of function of *let-60* by feeding RNA interference (RNAi) also partially suppressed *let-7(n2853)* in a reproducible manner. While 5% of *let-7* mutants grown on control RNAi survived at the nonpermissive temperature of 25°C (n = 302), 27% of *let-7(n2853); let-60(RNAi)* animals survived (n = 345) (Figures 2A and 2B). Thus, similar to other known *let-7* targets, *let-60* lf partially suppresses the *let-7(n2853)* lethal phenotype, suggesting that *let-7* lethality may at least partially be caused by overexpression of *let-60.* However *let-60(RNAi)* did not appear to suppress the *let-7* seam cell terminal differentiation defect and did not cause precocious seam cell terminal differentiation (data not shown). In addition, wild-type animals subjected to *let-60(RNAi)* did not display typical lethal and vulvaless phenotypes associated with *let-60* alleles (Beitel et al., 1990; Han et al., 1990; Han and Sternberg, 1990). Under our conditions, *let-60(RNAi)* resulted in ~80% knockdown of *let-60* mRNA (Grosshans et al., 2005), suggesting that the remaining *let-60* is still sufficient for seam cell differentiation and vulval development. To verify the specificity of the *let-60(RNAi)*, we showed that while *let-7(mn112)* adults all die, *let-60(n2021); let-7(mn112)* adults can live (see Experimental Procedures). Interestingly, *let-7(n2853); let-60(RNAi)* animals delivered a brood and could lay some eggs (data not shown), suggesting that the vulval-bursting phenotype of *let-7* was not suppressed merely because of the lack of a vulva.

*let-60* and *let-7* are both expressed in hypodermal seam cells (Dent and Han, 1998; Johnson et al., 2003). We fused the *let-60* 3′UTR behind the *Escherichia coli lacZ* gene driven by the hypodermally expressing *col-10* promoter (Figure 2C). We found that reporter gene activity is downregulated around the L4 stage (Figures 2D–2F), around the same time that *let-7* is expressed in the seam cells (Johnson et al., 2003). In contrast, the same reporter gene fused to an unregulated control 3′UTR was expressed at all stages (Figure 2F; Reinhart et al., 2000; Slack et al., 2000; Vella et al., 2004; Wightman et al., 1993). We found that reporter downregulation directed by the *let-60* 3′UTR depended on a wild-type *let-7* gene, since downregulation failed in *let-7(n2853)* mutants (Figure 2G). Thus, multiple lines of evidence strongly suggest that *let-60* is negatively regulated by *let-7*. First, the *let-60* 3′UTR contains multiple elements complementary to *let-7*; second, the *let-60* 3′UTR directs downregulation of a reporter gene in a *let-7* dependent manner; third, this downregulation is reciprocal to *let-7* upregulation in the hypodermis; and finally, *let-60* loss of function partially suppresses the *let-7* lethal phenotype.

### The *let-7* Family Member *mir-84* Is Dynamically Expressed in the Vulval Precursor Cells

*let-60/RAS* is best understood for its role in vulval development (Wang and Sternberg, 2001); however, *let-7* has not been reported to be expressed in the vulva. In *C. elegans*, *let-7*, *mir-48*, *mir-84*, and *mir-241* comprise the *let-7* family (Lau et al., 2001; Lim et al., 2003; Reinhart et al., 2000; Figures S1A and S1B). Our previous work demonstrated that a *let-7::gfp* fusion faithfully recapitulates the temporal expression of *let-7* and is temporally expressed in seam cell tissues affected in the *let-7* mutant (Johnson et al., 2003). We examined the expression pattern of *mir-84*, the closest *let-7* relative, by fusing 2.2 kilobases (kb) of genomic sequence immediately upstream of the miR-84 encoding sequence to the green fluorescent protein (*gfp*) gene. *mir-84::gfp* was first observed in the somatic gonad in larval stage 1 (L1). In L3 animals, strong expression was observed in uterine cells including the anchor cell (AC), and weak dynamic expression was observed in the vulval precursor cells (VPCs) (Figure 3). VPCs are multipotent ventral hypodermal cells that generate the vulva during L3 and later stages (Sulston and Horvitz, 1977). VPCs adopt one of three fates depending on EGF signaling from the AC (Wang and Sternberg, 2001; Figure 4H). The cell closest to the AC, P6.p, receives the most LIN-3/EGF signal (Katz et al., 1995) and adopts the primary (1°) fate through activation of a *RAS*/MAPK signal transduction pathway (Beitel et al., 1990; Han et al., 1990; Han and Sternberg, 1990); P5.p and P7.p receive less LIN-3 as well as receiving a secondary lateral signal (Sternberg, 1988) from P6.p and adopt the secondary (2°) fate; P3.p, P4.p, and P8.p adopt the uninduced tertiary (3°) fate. *mir-84::gfp* expression was observed during the early to mid L3 stage in all the VPCs except for P6.p, in which expression was rarely observed (Figures 3A,

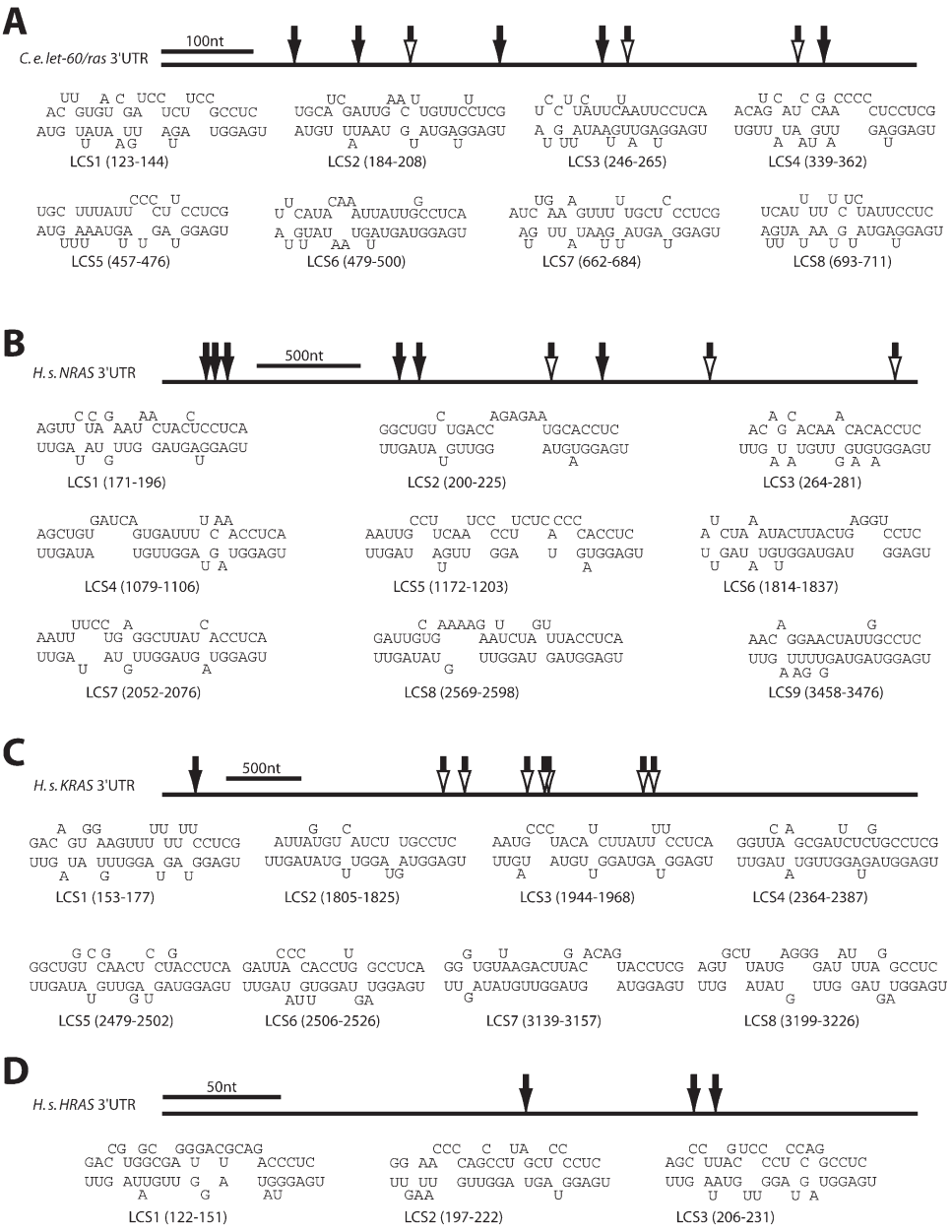


Figure 1. Potential LCSs in *C. elegans let-60/RAS* and in Mammalian *RAS* Genes

(A) *C. elegans let-60/RAS* mRNA 3′ UTR, black arrows indicate sites with similarity between *C.e.* and *C.b.* and white arrows indicate nonsimilar sites. Shown below are predicted duplexes formed by LCSs (top) and miR-84 (bottom). *let-7* and miR-84 are so similar that most *let-7* sites are also potential miR-84 sites.

(B–D), *H.s. NRAS*, *KRAS*, and *HRAS* mRNA 3′ UTRs have nine, eight, and three potential LCSs, respectively. Black arrows indicate sites conserved among mammalian species (in most cases human, rat, mouse, hamster, and guinea pig). Shown below are hypothesized duplexes formed by LCSs (top) and *let-7a* miRNA (bottom).

3P, S1C, and S1D). Subsequent VPC expression in the mid to late L3 stage was restricted to the daughters (Pn.px) of P5.p and P7.p with weaker GFP first appearing in the P6.p daughters just before their division into P6.pxx. Thereafter, equivalent expression was observed in the granddaughters (Pn.pxx) of P5.p, P6.p, and P7.p (Figures 3E and 3F). We note that *mir-84::gfp* expression was observed in all the VPCs except for P6.p at the stage when their fate in vulval development is determined by signaling from the AC (Figure 3O; Ambros, 1999), suggesting that *mir-84* could play a role in vulval cell fate determination. In the L4 stage, GFP expression was maintained in the AC and other uterine cells, appeared weakly in hypodermal seam cells (A.

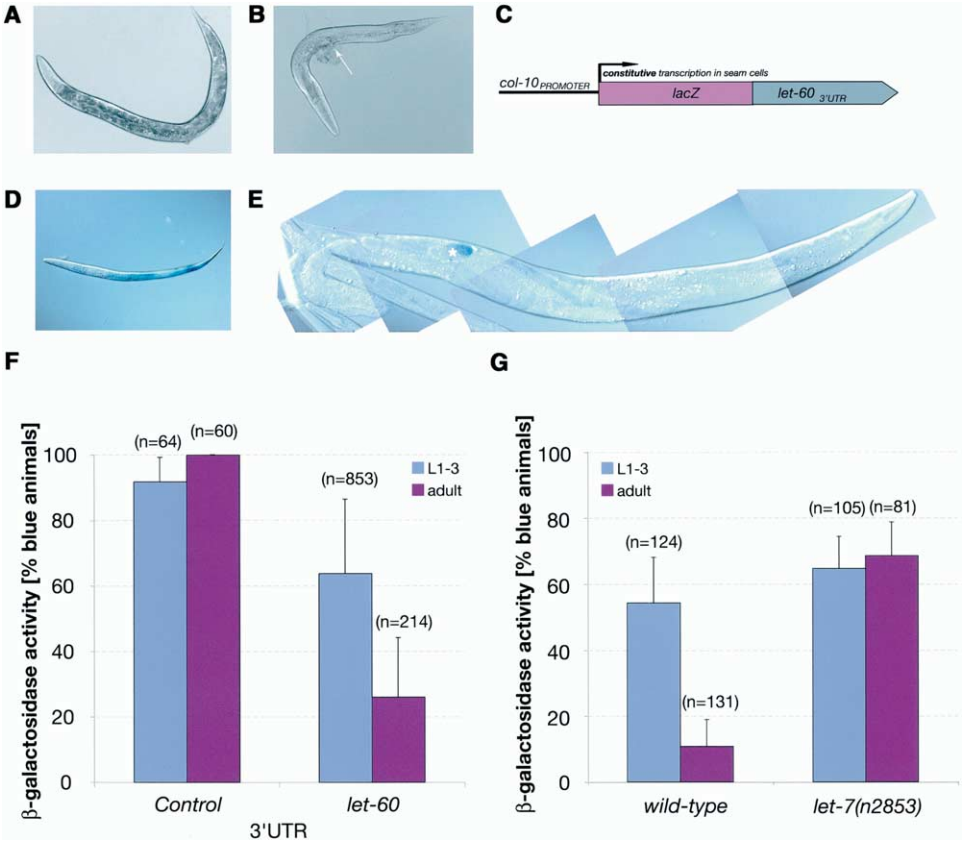


Figure 2. *let-60* Is Regulated by the *let-7* miRNA through Its 3′ UTR

(A) Many *let-7(n2853); let-60(RNAi)* mutant animals do not burst through the vulva at the adult stage at the restrictive temperature (25°C), while all *let-7(n2853)* animals do (B).

(C–E) Wild-type animals carrying a reporter gene schematically shown in (C) show robust hypodermal expression of β-galactosidase at the L1 stage ([D], magnification 400×) but not at the adult stage ([E], composite of multiple images shot at 400×). Asterisk in (E) indicates an embryo with β-galactosidase activity inside the adult animal, providing an internal control for staining.

(F) Quantitative analysis of the expression pattern from five independent wild-type transgenic lines grown at 20°C. We observed at least 25% repression in all lines. A nonregulated *lin-41* 3′ UTR missing its LCSs (pFS1031) (Reinhart et al., 2000), tested in duplicate is shown as a control.

(G) Downregulation of the reporter gene expression is lost in *let-7(n2853)* mutant worms grown at the permissive temperature, 15°C. The parental (N2) line was tested in triplicate; four isogenic *let-7(n2853)* mutant lines were tested. Error bars represent standard deviations.

Kerscher et al., submitted), and was upregulated to higher levels in many P5.p–P7.p descendants (Figure 3G). Interestingly, a second *let-7* family member, *mir-48*, was also expressed in non-P6.p VPCs (A. Kerscher et al., submitted), suggesting the potential for redundancy between *mir-48* and *mir-84* in the VPCs.

### *mir-84* Overexpression Causes Vulval and Seam Defects

We overexpressed miR-84 by generating transgenic animals harboring a multicopy array of a 3.0 kb genomic DNA fragment that spans from 2.2 kb upstream to 0.8 kb downstream of the miR-84 encoding sequence (called *mir-84*(+++)). These animals expressed elevated levels of miR-84 (Figure 4G) and displayed abnormal vulval development phenotypes, including protrusion and bursting of the vulva (40% of animals, n = 40; Figure 4B). They also displayed early division of P6.p and precocious vulval invagination in mid to late L3, a heterochronic phenotype we have not investigated further (Figure 4A). Consistent with *mir-84::gfp* expression in seam cells, we found that *mir-84*(+++) animals also exhibited precocious seam cell terminal differentiation and alae formation in the L4 stage (Figure 4C), a characteristic seen in precocious developmental timing mutants. In fact, *let-7* overexpressing strains also exhibit precocious seam cell terminal differentiation in the L4 stage (Reinhart et al., 2000). In contrast, animals carrying an array containing a construct identical to *mir-84*(+++) except for a 75 nucleotide (nt) deletion of sequences encoding the predicted pre-*mir-84* (Δ*mir-84*(+++)) did not display any vulval or seam defects (data not shown), demonstrating that the phenotypes observed in *mir-84*(+++) are dependent on the miR-84 sequence.

We searched for LCSs in the 3′ UTRs of all genes known to play a role in vulval development (Table S1). LCSs have the potential to bind all members of the *let-7* family, including *mir-84*. Approximately 11 vulval genes contained at least one LCS (Table S1), raising the possibility that the *let-7* family may regulate multiple genes in the vulva. In this analysis though, *let-60/RAS* stood out due to the high number of LCS sites.

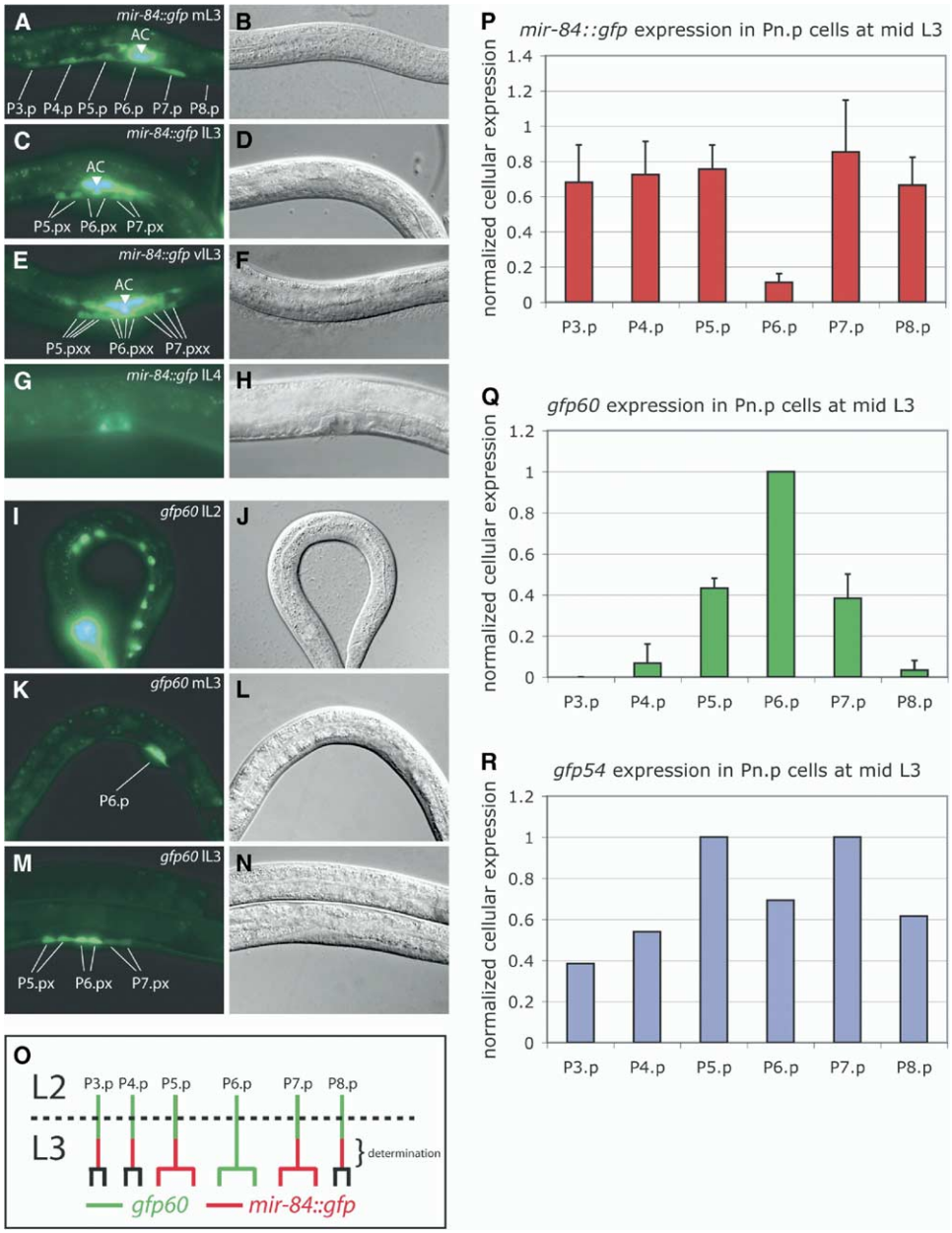


Figure 3. *mir-84::gfp* and *gfp60* Are Expressed Reciprocally in the Pn.p Cells

(A, C, E, and G) In L3, *mir-84::gfp* is expressed in all Pn.p cells except P6.p during the time of vulval fate determination ([O], bracket) and is upregulated in P6.pxx cells thereafter (mL3, lL3, and vlL3 are mid, late, and very late L3, respectively).

(I, K, and M) *gfp60*, a fusion of *gfp* to the *let-60* 3′UTR, driven by the *lin-31* promoter, is expressed in all Pn.p cells at late L2 and early L3 (I and J), is then restricted to P6.p (K and L) during vulval fate determination, and thereafter is expressed strongly in P6.px cells and weakly in P5.px and P7.px cells (M and N). Images on right are Nomarski images of animals on left.

(O) *gfp60* and *mir-84::gfp* expression schematic from L2 Pn.p to mid L3 Pn.px.

(P–R), Quantification of expression data shown in (A–N). *gfp54* is a fusion of *gfp* to the *unc-54* 3′UTR, driven by the *lin-31* promoter. Error bars represent standard deviations. See Experimental Procedures for details.

### *mir-84* Overexpression Partially Suppresses *let-60/RAS* Gain of Function Phenotypes

*let-60/RAS* is active in P6.p following a *lin-3* EGF signal from the anchor cell that activates a MAPK signal transduction cascade transforming P6.p to the 1° vulval fate (Han and Sternberg, 1990). Since *mir-84* is expressed in all VPCs except P6.p, we examined the possibility that *mir-84* negatively regulates expression of *let-60/RAS* in cells not destined to adopt the 1° fate. Activating mutations in *let-60/RAS* cause multiple VPCs (including the non-P6.p VPCs) to adopt 1° or 2° fates leading to a multivulva (Muv) phenotype (Han et al., 1990). We found that overexpression of *mir-84* partially suppressed the Muv phenotype of *let-60(gf)* mutations. In our study 41% (n = 51) of *let-60(ga89)* (Eisenmann and Kim, 1997) animals displayed a Muv phenotype, while

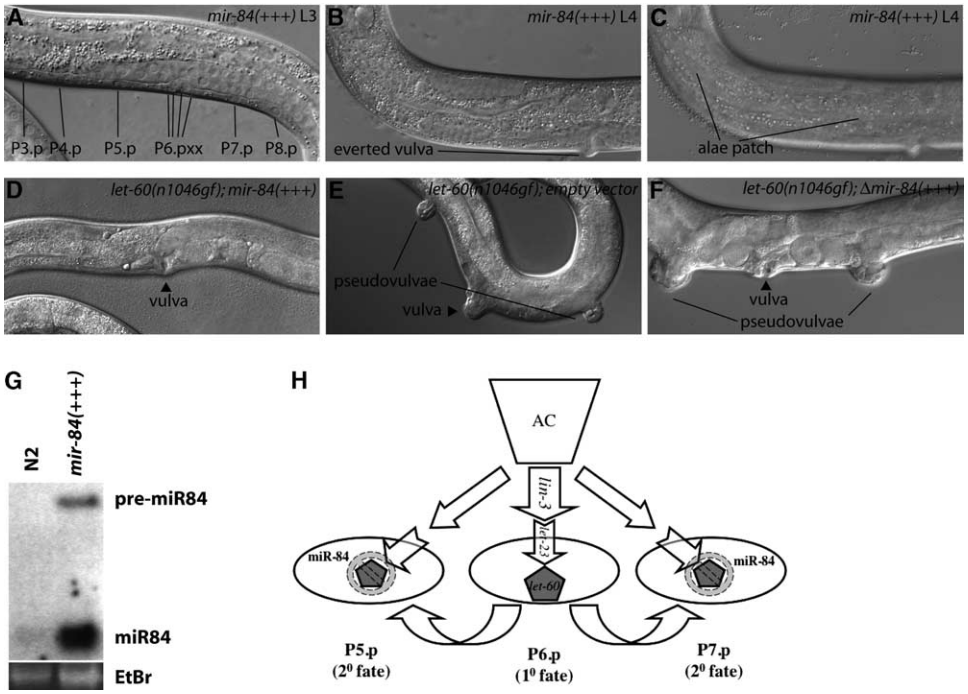


Figure 4. Overexpression of *mir-84*

In L3, *mir-84*(+++) animals display precocious division of P6.p and precocious vulval invagination (A). In L4, *mir-84*(+++) results in an everted and protruding vulva (B) and precocious alae formation (C).

(D–F), Overexpressing *mir-84* in *let-60(n1046gf)* animals partially suppresses the *let-60(gf)* Muv phenotype, whereas an empty vector control and Δ*mir-84*(+++) do not.

(G), Northern blot showing that *mir-84*(+++) animals express more miR-84, compared to wild-type animals. 5.8S RNA is shown as a loading control.

(H), Model of miR-84 modulation of *let-60/RAS* during vulval morphogenesis. During vulval cell fate specification a LIN-3/EGF signal emanating from the anchor cell is received by the LET-23/EGFR on the P5.p, P6.p and P7.p cells. The P6.p receives the most LIN-3 and activates a RAS/MAPK signal transduction pathway to adopt the 1° fate. P5.p and P7.p receive less LIN-3 and also receive a second, lateral signal (involving LIN-12/Notch) from the 1° cell that induces them to the 2° fate. We propose that miR-84 is expressed in the non-1° lineage to reduce expression of LET-60/RAS in these cells.

only 13% (n = 168) did so when also overexpressing *mir-84* from a multicopy array (p << 0.0001, chi-square test). The same suppression was observed with a second *let-60(gf)* allele, *let-60(n1046)* (Han et al., 1990): 77% (n = 39) of *let-60(n1046)* animals displayed a Muv phenotype (Figure 4E), while only 50% (n = 113) did so when also overexpressing *mir-84* (Figure 4D; p << 0.0001, chi-square test). *let-60(n1046)* animals displayed an average of 1.54 pseudovulvae per animal compared to an average of 0.66 pseudovulvae per *let-60(n1046)* animal overexpressing *mir-84*. For both *let-60(gf)* alleles, animals exhibiting low mosaicism for the *myo-3::gfp* coinjection marker were completely suppressed (data not shown), suggesting that the partial suppression was likely due to mosaicism of the transgeneic array. Neither an empty vector control (TOPO) (n = 111; p = 0.1435, chi-square test) nor the Δ*mir-84*(+++) array (n = 129; Figure 4F), suppressed the Muv phenotype of *let-60(n1046*). For all *let-60(gf)* experiments, three independent lines behaved similarly (Figure S3C).

### The *let-60/RAS* 3′UTR Confines Expression to P6.p

The promoter of *let-60/RAS* drives reporter expression in all VPCs (Dent and Han, 1998). However, the transgenic reporters used in this earlier work did not include the *let-60* 3′UTR. We fused GFP to the *let-60* 3′UTR and drove GFP expression in all the VPCs using the VPC-specific *lin-31* (Tan et al., 1998) promoter (*gfp60)*. In the late L2 and early L3 stages, GFP was expressed in all the Pn.p cells (Figure 3I), but by mid to late L3 stages, GFP was largely restricted to the P6.p cell (Figures 3K and 3Q), with some expression in the P5.p and P7.p cell descendants (Figure 3M). A similar fusion construct in which the *let-60* 3′UTR was replaced by the unregulated *unc-54* 3′UTR showed GFP expression in all Pn.p cells (Figure 3R). Since the *lin-31* promoter is active in all Pn.p cells (Tan et al., 1998), this result demonstrates that the *let-60/RAS* 3′UTR is sufficient to downregulate a reporter gene in the non-P6.p cells.

We replaced the *let-60* 3′UTR with the unregulated *unc-54* 3′UTR in a *let-60* genomic DNA fragment. While we could generate viable lines using a *let-60::let-60(+)::let-60* 3′UTR construct at 10 ng/μl (data not shown), we were unable to generate viable transformants using this *let-60::let-60(+)::unc-54* 3′UTR construct, even at 0.1 ng/μl. We did not try lower concentrations of DNA, but our result suggests that the removal of the *let-60* 3′UTR may severely overexpress *let-60* and cause lethality.

### *let-60/RAS* Is a Likely Target of *mir-84* in the Vulva

Previous work has demonstrated that VPCs are sensitive to the levels of *let-60/RAS* (Beitel et al., 1990; Han and Sternberg, 1990). Animals carrying extra copies of the wild-type *let-60/RAS* gene display a Muv phenotype, where non-P6.p VPCs can adopt the 1° fate. Our data strongly suggest that *mir-84* negatively regulates *let-60* in non-P6.p VPCs. First, *mir-84* is complementary to multiple sites in the *let-60* 3′UTR. Second, *mir-84* is expressed in a reciprocal manner to *let-60* in the VPCs. miR-84 is largely absent from P6.p, at the same time as the *let-60* 3′UTR confines GFP expression mainly to the P6.p cell lineage. Finally, *mir-84* overexpression partially suppresses the effects of activating mutations in the *let-60* gene. We propose that *mir-84* modulates the expression of *let-60/RAS* in non-P6.p VPCs to reduce flux through the RAS/MAPK signaling pathway and hence decrease the likelihood that these cells will also adopt the 1° fate (Figure 4H). However, *mir-84* is clearly not the only regulator of *let-60/RAS* in non-P6.p cells: *daf-12(rh61)* mutants do not express *mir-84* in any VPC (n = 60 animals), and yet *daf-12(rh61)* animals do not display a Muv phenotype (data not shown). Other known factors, e.g., *synmuv* genes (Berset et al., 2001; Ceol and Horvitz, 2004; Hopper et al., 2000; Lee et al., 1994; Wang and Sternberg, 2001; Yoo et al., 2004; Yoon et al., 1995) or unknown factors may also regulate *let-60/RAS* signaling in these cells.

Our combined results provide strong evidence that *let-7* and *mir-84* regulate *let-60/RAS* expression through its 3′UTR in seam and vulval cells, cells in which they are all naturally expressed. Given that the 3′UTR of *let-60/RAS* contains multiple *let-7/mir-84* complementary sites, we propose that this regulation is direct.

### *let-7* Complementary Sites in Human *RAS* 3′UTRs

Numerous miRNAs are altered in human cancers (Calin et al., 2002; Calin et al., 2004; Michael et al., 2003; Tam et al., 2002) and three of the best understood miRNAs, *lin-4* (Lee et al., 1993), *let-7* (Reinhart et al., 2000), and *bantam* (Brennecke et al., 2003), all regulate cell proliferation and differentiation. The closest human homologs of *let-7* and *mir-84* are the *H.s. let-7* family miRNAs (Lagos-Quintana et al., 2002; Pasquinelli et al., 2000). *let-60/RAS* is the *C. elegans* ortholog of human *HRAS*, *KRAS*, and *NRAS* (Figures S3A and S3B), which are commonly mutated in human cancer (Malumbres and Barbacid, 2003), including lung cancer. We found that all three human *RAS* 3′UTRs contain multiple putative *let-7* complementary sites with features of validated *C. elegans* LCSs (Figures 1B, 1C, and 1D). Many of these are conserved in rodents, amphibians, and fish (Figure S4), suggesting functional relevance. The presence of putative LCSs in human *RAS* 3′UTRs suggests that mammalian *let-7* family members may regulate human *RAS* in a manner similar to the way *let-7* and *mir-84* regulate *let-60/RAS* in *C. elegans.*

### Human *RAS* Expression Is regulated by *let-7* in Cell Culture

Microarray analysis on six different cell lines revealed that HepG2 cells express *let-7* at levels too low to detect by microarray analysis (data not shown). We transfected HepG2 cells with a double-stranded (ds) RNA that mimics the *let-7a* precursor. A similar approach has been used to study other miRNAs in mammalian cells (Chen et al., 2004; Lewis et al., 2003). Consistent with the prediction that RAS expression is negatively regulated by *let-7*, immunofluorescence with a RAS-specific antibody revealed that the protein is reduced by approximately 70% in HepG2 cells transfected with exogenous *let-7a* miRNA relative to the same cells transfected with a negative control miRNA (Figures 5A and 5B). The protein expression levels of GAPDH and $p21^{CIP1}$ were largely unaffected by the transfected *let-7a* and negative control pre-miRNAs (Figures S5A and S5B), indicating that *let-7a* regulation is specific to RAS. To confirm that the RAS antibody is specific to RAS protein in the transfected cells, HepG2 cells were also independently transfected with two exactly complementary siRNAs targeting independent regions of *NRAS*. Both siRNAs reduced cell fluorescence by more than 60% as compared to negative control siRNA-transfected cells (Figures S5C and S5D).

We predicted that cells expressing native *let-7* may express less RAS protein and that inhibition of *let-7* may lead to derepression of RAS expression. To test this, we transfected HeLa cells, which express endogenous *let-7* (Lagos-Quintana et al., 2001; Lim et al., 2003), with antisense molecules designed to inhibit the activity of *let-7* (Hutvágner et al., 2004; Meister et al., 2004). Reducing the activity of *let-7* in HeLa cells resulted in an ~70% increase in RAS protein levels (Figures 5C and 5D). These results, combined with the reciprocal experiment using pre-*let-7* miRNAs discussed above, strongly suggest that *let-7* negatively regulates the expression of RAS in human cells.

We fused the 3′UTR of human *NRAS* and *KRAS* to a luciferase reporter gene and transfected these constructs along with transfection controls into HeLa cells. *NRAS* contains two naturally occurring 3′UTRs that utilize alternative polyadenylylation and cleavage sites, such that one of the 3′UTRs is 2.5 kb longer than the other. We found that while the long *NRAS* 3′UTR strongly repressed reporter expression compared to an unregulated control 3′UTR (Figures 6A and 6B), the short *NRAS* 3′UTR led to only slight, but reproducible, repression of the reporter. The short 3′UTR contains four LCSs, while the long form contains nine LCSs. The *KRAS* 3′UTR also repressed the luciferase reporter (Figures 6A and 6B), while *HRAS* was not tested. Our results demonstrate that the 3′UTRs of *NRAS* and *KRAS* contain regulatory information, sufficient to downregulate the reporter. Little is known about the exact characteristics that convey functionality to a miRNA complementary site, and future work may reveal the differences between the *NRAS* and *KRAS* 3′UTRs.

As with the endogenous *RAS* experiments described above, we performed the reciprocal experiment wherein we cotranfected HeLa cells with the *RAS* 3′ UTR reporter constructs and the *let-7a* antisense inhibitor molecule (or a control scrambled molecule). Cells transfected with the *let-7a* inhibitor relieved repression exerted on the reporter relative to the control transfections (Figure 6C). Since we observe a loss in the extent

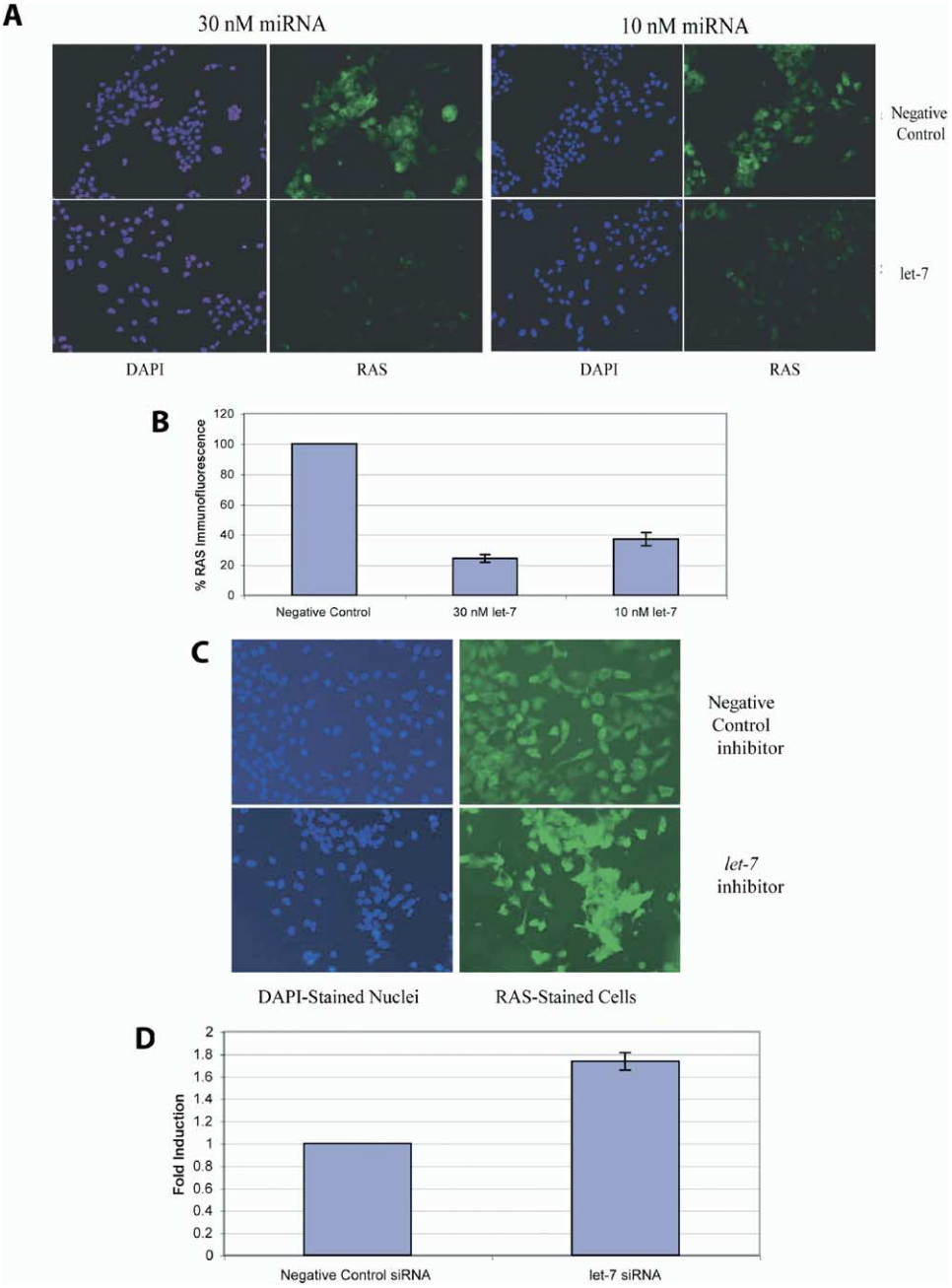


Figure 5. The Presence of *let-7* Influences the Expression of *RAS* in Human Cells

(A) HepG2 cells were transfected with 10 and 30 nM of a *let-7* or negative control precursor miRNA. Immunofluorescence using an antibody specific to NRAS, VRAS, and KRAS revealed that the *let-7* transfected cells have much lower levels of the RAS proteins.

(B) Quantification of the RAS antibody fluorescence from replicates of the transfections shown in (A).

(C) HeLa cells were transfected with 100 nM *let-7* inhibitor or negative control inhibitor. RAS immunofluorescence revealed that cells transfected with the *let-7* inhibitor have increased levels of the RAS proteins relative to the negative control transfected cells.

(D) Quantification of the RAS antibody fluorescence from replicates of the transfections shown in (C).

of downregulation when *let-7* is inhibited, these results strongly suggest that *let-7* regulates *NRAS* and *KRAS* in human cells through their 3′ UTRs.

### *let-7, RAS*, and Lung Cancer

Like *let-60/ras*, human *RAS* is dose sensitive, since overexpression of *RAS* results in oncogenic transformation of human cells (McKay et al., 1986; Pulciani et al., 1985). It is plausible that loss of miRNA control of *RAS* could also lead to overexpression of *RAS* and contribute to human cancer. Indeed, recent work has mapped *let-7* family members to human chromosomal sites implicated in a variety of cancers (Calin et al., 2004). In particular *let-7a-2, let-7c* and *let-7g* have been

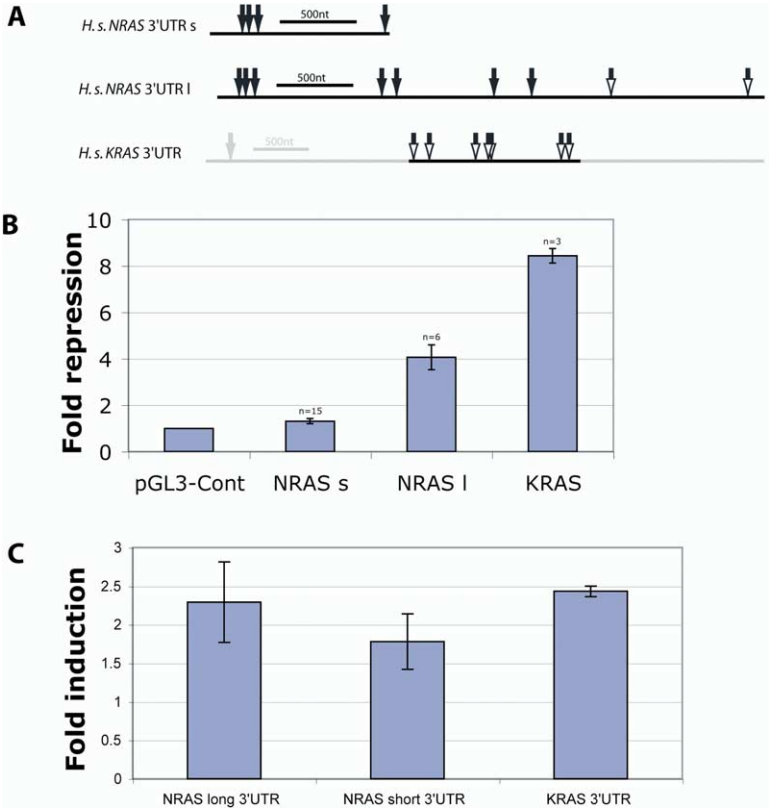


Figure 6. The 3′ UTRs of NRAS and KRAS Enable *let-7* Regulation

(A) Cartoon showing the *NRAS* short (NRAS s) *NRAS* long (NRAS l) and *KRAS* 3′ UTRs. Arrows indicate LCSs as described in Figure 1. The blackened areas indicate the sequence cloned behind the reporter.

(B) Relative repression of firefly luciferase expression standardized to a transfection control, renilla luciferase. pGL3-Cont is the empty vector.

(C) Induction of firefly luciferase expression when reporter plasmids with 3′ UTR domains corresponding to KRAS and NRAS are co-transfected with an inhibitor of *let-7*, relative to a control inhibitor.

linked to small chromosomal intervals that are deleted in lung cancers (Calin et al., 2004), a cancer type in which *RAS* misregulation is known to be a key oncogenic event (Ahrendt et al., 2001; Johnson et al., 2001).

We utilized a miRNA microarray to examine expression levels of members of the *let-7* gene family in tissue from 21 different cancer patients, including 12 lung cancer patients with squamous cell carcinomas (stage IB or IIA). We found that the *let-7* miRNAs were reduced in expression in a number of the tumors relative to the normal adjacent tissue (NAT) samples from the same patients (Figure 7A). Interestingly, we found that *let-7* was expressed at lower levels in all of the lung tumor tissues (Figure 7) but only sporadically in other tumor types. A similar finding was independently discovered (Takamizawa et al., 2004). On average, *let-7* was expressed in lung tumors at less than 50% of what it was expressed in the associated normal lung samples (Figure 7A). We used Northern analysis to measure *let-7c* in the tumor and NAT samples for the two patients from which we purified enough RNA (samples represented by the first and fifth lung cancer bars in Figure 7A). Consistent with the microarray results, Northern analysis verified that the expression of *let-7c* was 65% lower in the tumor of patient 1 and 25% lower in the tumor of patient 5 (Figure 7B). Seven of eight examined samples also had on average 30% less *let-7g* expression in the tumor tissue (Figure S6). The miRNA arrays used to compare the lung tumors and NAT included probes for 167 total miRNAs; the expression of the vast majority of these were unchanged in the lung tumors (J.S. and D.B., unpublished data) indicating that *let-7* might be important in lung cancer. In theory, downregulation of *let-7* could result in upregulation of RAS and thus induce or accentuate oncogenesis.

To test this hypothesis, we isolated total RNA and total protein from the tumor and normal adjacent tissues of three new lung cancer patients with squamous cell carcinoma. The RNA samples were split and half was used for Northern analysis to measure *let-7c* and U6 snRNA. The other halves of the RNA samples were used for real-time PCR to measure the *NRAS* mRNA, 18S rRNA, and B-actin mRNA. The protein samples were used for Western analysis to assess RAS and GAPDH protein levels. As seen in Figure 7C, RAS protein was present in the tumors at levels at least 10-fold higher than in the normal adjacent samples from the same patients. Consistent with the miRNA array results for other lung cancer samples, all three lung tumor samples had 4- to 8-fold lower levels of *let-7* than did the corresponding NAT samples. Interestingly, the first and third lung cancer samples had similar levels of *NRAS* mRNA in both the tumor and NAT while the second sample pair had significantly higher levels of *NRAS* mRNA in the tumor sample. In our limited analysis, RAS protein levels correlate poorly with *NRAS* mRNA levels but very well with *let-7* levels, suggesting that the expression of the oncogene is significantly influenced at the level of translation, consistent with the known mechanism of *let-7* in invertebrates.

The reciprocal expression pattern between *let-7* and RAS in cancer cells closely resembles what we saw

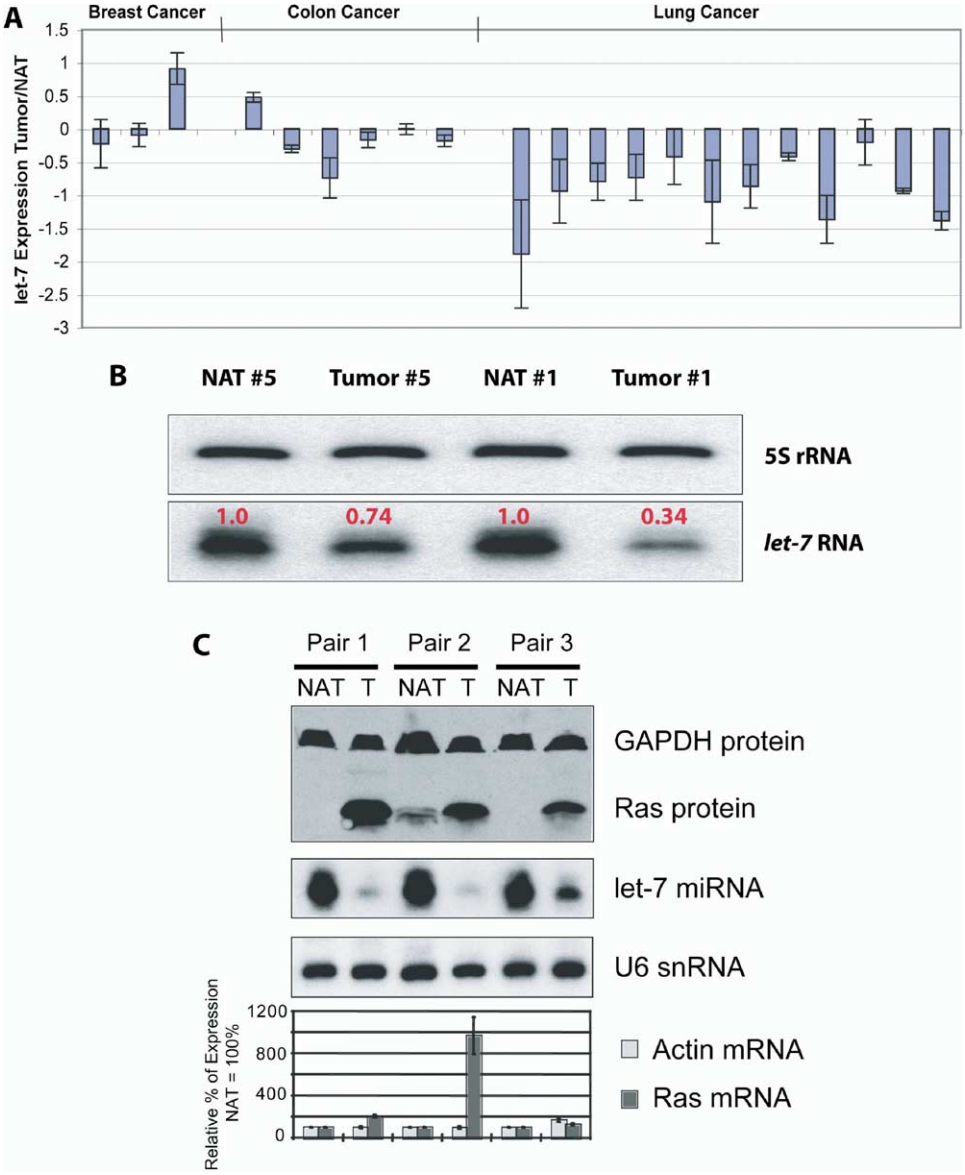


Figure 7. *let-7* Is Poorly Expressed in Lung Tumors

(A) Expression of *let-7* in 21 breast, colon, and lung tumors relative to associated NAT. Fluorescently labeled miRNA was hybridized to microarrays that included probes specific to *let-7a* and *let-7c*. Fluorescence intensities for the tumor and NAT were normalized by total fluorescence signal for all elements, and the relative average signal from the *let-7* probes in the tumor and normal adjacent samples are expressed as log ratios. Note, *let-7a* and *let-7c* had similar profiles, suggesting crosshybridization between the two closely related miRNAs.

(B) Confirmation of differential *let-7c* expression in tumor versus normal adjacent samples. The Northern blot was assayed sequentially with radio-labeled probes specific to *let-7c* and 5S rRNA. The relative expression of *let-7c* in NAT versus tumor tissue, normalized to the 5S signal, is shown in patients corresponding to lung sample 1 and 5 from (A).

(C) Correlation between RAS protein and *let-7c* expression in tumor and normal adjacent tissue samples from three lung squamous cell carcinomas. GAPDH and RAS proteins were measured from crude extracts of tumor and normal adjacent tissues using Western analysis. The two proteins were assessed simultaneously by mixing the antibodies used for detection. The small RNA Northern blot was assayed sequentially with radio-labeled probes specific to *let-7c* and U6 snRNA. *NRAS* mRNA in the tumor and normal adjacent tissues samples was measured by real-time PCR. The real-time data were normalized based on the real-time PCR detection of 18S rRNA in the various samples. The relative expression of *NRAS* in the normal adjacent tissues was taken to be 100%, and the Ct value of *NRAS* in the tumor samples was used to assign the relative expression of *NRAS* in the tumor samples.

with *let-7* and RAS in *C. elegans* and in our human tissue culture experiments. The correlation between reduced *let-7* expression and increased RAS protein expression in the lung tumor samples suggests that one or more members of the *let-7* gene family regulates *RAS* expression in vivo and that the level of expression of the miRNA might be an important factor in limiting or contributing to oncogenesis.

## Conclusions

Our work reveals that the *let-7* miRNA family negatively regulates *RAS* in two different *C. elegans* tissues and in two different human cell lines. Strikingly, *let-7* is expressed in normal adult lung tissue (this work; Pasquinelli et al., 2000) but is poorly expressed in lung cancer cell lines and lung cancer tissue (this work; Takamizawa et al., 2004). The expression of *let-7* inversely correlates with expression of RAS protein in lung cancer tissues, suggesting a possible causal relationship. In addition, overexpression of *let-7* inhibited growth of a lung cancer cell line in vitro (Takamizawa et al., 2004), suggesting a causal relationship between *let-7* and cell growth in these cells. The combined observations that *let-7* expression is reduced in lung tumors, that several *let-7* genes map to genomic regions that are often deleted in lung cancer patients, that overexpression of *let-7* can inhibit lung tumor cell line growth, that the expression of the *RAS* oncogene is regulated by *let-7*, and that RAS is significantly overexpressed in lung tumor samples strongly implicate *let-7* as a tumor suppressor in lung tissue and suggests a possible mechanism.

## Experimental Procedures

### Plasmid Constructs

See Supplemental Experimental Procedures for details of plasmid construction.

### *C. elegans* and Transgenic Reporter Analysis

All animal experiments were performed at room temperature or 20°C unless stated otherwise. All experimental plasmids were injected in animals at 50–100 ng/μl. Two different markers, *rol-6* (100 ng/μl) and *myo-3::gfp* (50 ng/μl), were separately coinjected with PSJo84. *myo-3::gfp* (50 ng/μl) was coinjected with o84Δ84, and *myo-2::gfp* (5 ng/μl) was coinjected with GFP60 and GFP54. These animals are mosaic for the transgenes. To compare expression between individual lines, the percent expression of GFP in each of the Pn.p cells was normalized relative to the expression of the highest expressing Pn.p cell and represented as a fraction of the highest expresser for each individual line of animals. For each construct, the average of the lines was calculated along with the standard deviation for each construct represented as error bars (*mir-84::gfp* n = 239, *gfp60* n = 42 and *gfp54* n = 40). For the *mir-84*(+++) analysis, animals were examined using DIC optics to score seam cell and vulval anatomy. LacZ reporter analysis was as described (Vella et al., 2004). The *lin-41 3UTR* missing its LCSs (pFS1031) was used as a control (Reinhart et al., 2000). RNAi methods were standard feeding procedures using synchronized L1s (Timmons et al., 2001). All RNAi experiments were done in parallel to an empty vector (L4440) feeding control. See Supplemental Experimental Procedures for details on the *let-60; let-7* double mutant cross.

### *let-7*/*RAS* Association in Mammalian Cells

HeLa S3 cells grown in D-MEM (GIBCO) supplemented with 10% fetal bovine serum (GIBCO) were cotransfected in 12-well plates using Lipofectamine 2000 (Invitrogen) according to the manufacturer's protocol using 1.0 μg/well of *Pp*-luc-expressing plasmid (pGL3-Control from Promega, pGL3-NRAS S pGL3-NRAS L and pGL3-KRAS) and 0.1 μg/well of *Rr*-luc-expressing plasmid (pRL-TK from Promega). 24 hr posttransfection, the cells were harvested and assayed using the Dual Luciferase assay as described by the manufacturer (Promega). HeLa cells grown as above were transfected in 24-well plates with 30 pmol of Anti-miR *let-7* or negative control 1 inhibitors (Ambion) using Lipofectamine 2000. Three days posttransfection, RAS expression was monitored by immunofluorescence using an FITC conjugated primary antibody against RAS protein (US Biological). The resulting fluorescent signal was analyzed using the appropriate filter set and was quantified using MetaMorph software. We typically measured the fluorescence intensity of 150–300 cells in one or a few viewing areas. The experiments with both the precursors and the inhibitors were performed three times. The photos represent single viewing fields from one of the experiments and are representative of the triplicate experiment. Identically grown HeLa cells were cotransfected in 24-well plates using Lipofectamine 2000 (Invitrogen) according to the manufacturer's protocol using 200 ng /well of *Pp*-luc-expressing plasmid (pGL3-Control from Promega, pGL3-NRAS S pGL3-NRAS L and pGL3-KRAS). 48 hr posttransfection, the cells were harvested and assayed using the Luciferase assay as described by the manufacturer (Promega).

HepG2 cells grown in D-MEM (GIBCO) supplemented with 10% fetal bovine serum (GIBCO) were transfected with 15 or 5 pmol of Pre-miR *Let-7c* or negative control 1 Precursor miRNAs (Ambion) in 24-well plates using siPort Neo-FX (Ambion) according to the manufacturer's protocol. Three days posttransfection, RAS expression was monitored by immunofluorescence as described above.

### MiRNA Microarray Analysis

Total RNA from tumor and NAT samples from three breast cancer, six colon cancer, and twelve lung cancer patients was isolated using the mirVana RNA Isolation Kit (Ambion). Twenty micrograms of each total RNA sample was fractionated by polyacrylamide gel electrophoresis (PAGE) using a 15% denaturing polyacrylamide gel, and the miRNA fractions for each sample were recovered. The miRNAs from all of the samples were subjected to a poly(A) polymerase reaction wherein amine modified uridines were incorporated as part of ~40 nt long tails (Ambion). The tailed tumor samples were fluorescently labeled using an amine-reactive Cy3 (Amersham), and the normal adjacent tissue samples were labeled with Cy5 (Amersham). The fluorescently labeled miRNAs were purified by glass-fiber filter binding and elution (Ambion), and the tumor and normal adjacent tissue samples from the same patient were mixed. Each sample mixture was hybridized for 14 hr with slides upon which 167 miRNA probes were arrayed. The microarrays were washed 3 × 2 min (min) in 2× SSC and scanned using a GenePix 4000B (Axon). Fluorescence intensities for the Cy3- and Cy5-labeled samples for each element were normalized by total Cy3 and Cy5 signal on the arrays. The normalized signal intensity for each element was compared between the tumor and NAT samples from each pair of patient samples and expressed as a log ratio of the tumor to normal adjacent sample.

### Northern Analysis

*mir-84* Northerns were performed as described (Johnson et al., 2003). For human tissues, 1 μg of total RNA from the tumor and normal adjacent tissues of patients 1 and 5 (Figure 7A) were fractionated by PAGE using a 15% denaturing polyacrylamide gel. The RNA was transferred to a positively charged nylon membrane by electroblotting at 200 mA in 0.5× TBE for 2 hr. The Northern blot was dried and then incubated overnight in 10 ml of ULTRAhyb-Oligo (Ambion) with $10^7$ cpm of a radio-labeled transcript complementary to *let-7c*. The blot was washed 3 × 10 min at room temperature in 2× SSC, 0.5% SDS and then 1 × 15 min at 42°C in 2× SSC, 0.5% SDS. Overnight phosphorimaging using the Storm system (Amersham) revealed *let-7c*. The process was repeated using a radio-labeled probe for 5S rRNA.

### Lung Tumor Protein/Northern/mRNA Analysis

Total RNA and protein were isolated from tumor and normal adjacent tissue samples from three lung cancer patients using the mirVana PARIS Kit (Ambion). *let-7* miRNA and U6 snRNA were measured using the Northern procedure described above. NRAS and B-actin mRNA as well as 18S rRNA were quantified by real-time RT-PCR using primers specific to each of the target RNAs. RAS and GAPDH protein were measured by Western analysis using the

RAS antibody described above and an antibody for GAPDH (Ambion).

### Supplemental Data

Supplemental Data include six figures, one table, and Supplemental Experimental Procedures and can be found with this article online at http://www.cell.com/cgi/content/full/120/5/635/DC1/.

### Acknowledgments

We thank S. Kim for the *lin-31* promoter (PB255), T. Johnson and M. Gerstein for help with the computational analysis, A. Fire for pPD95.70, the *Caenorhabditis* Genetics Stock Center for strains, and K. Jeffers and J. Shelton for technical and intellectual contributions. We thank R. Goetsch, S. Hartman, and M. Snyder for HeLa S3 cells and D. Banerjee, K. Carter, and M. Stern for critical reading of this manuscript. H.G. was supported by a long-term fellowship from the Human Frontiers Science Program. F.J.S. was supported by NIH grant (GM62594) and NSF grant (IBN-03444429).

Received: September 2, 2004
Revised: January 5, 2005
Accepted: January 12, 2005
Published: March 10, 2005

### References

Abrahante, J.E., Daul, A.L., Li, M., Volk, M.L., Tennessen, J.M., Miller, E.A., and Rougvie, A.E. (2003). The *Caenorhabditis elegans* hunchback-like gene *lin-57/hbl-1* controls developmental time and is regulated by microRNAs. Dev. Cell *4*, 625–637.

Ahrendt, S.A., Decker, P.A., Alawi, E.A., Zhu Yr, Y.R., Sanchez-Cespedes, M., Yang, S.C., Haasler, G.B., Kajdacsy-Balla, A., Demeure, M.J., and Sidransky, D. (2001). Cigarette smoking is strongly associated with mutation of the *K-ras* gene in patients with primary adenocarcinoma of the lung. Cancer *92*, 1525–1530.

Ambros, V. (1999). Cell cycle-dependent sequencing of cell fate decisions in Caenorhabditis elegans vulva precursor cells. Development *126*, 1947–1956.

Bartel, D.P. (2004). MicroRNAs: Genomics, biogenesis, mechanism, and function. Cell *116*, 281–297.

Beitel, G.J., Clark, S.G., and Horvitz, H.R. (1990). Caenorhabditis elegans *ras* gene *let-60* acts as a switch in the pathway of vulval induction. Nature *348*, 503–509.

Berset, T., Hoier, E.F., Battu, G., Canevascini, S., and Hajnal, A. (2001). Notch inhibition of RAS signaling through MAP kinase phosphatase LIP-1 during C. elegans vulval development. Science *291*, 1055–1058.

Brennecke, J., Hipfner, D.R., Stark, A., Russell, R.B., and Cohen, S.M. (2003). *bantam* encodes a developmentally regulated microRNA that controls cell proliferation and regulates the proapoptotic gene *hid* in *Drosophila*. Cell *113*, 25–36.

Calin, G.A., Dumitru, C.D., Shimizu, M., Bichi, R., Zupo, S., Noch, E., Aldler, H., Rattan, S., Keating, M., Rai, K., et al. (2002). Frequent deletions and down-regulation of micro- RNA genes *miR15* and *miR16* at 13q14 in chronic lymphocytic leukemia. Proc. Natl. Acad. Sci. USA *99*, 15524–15529.

Calin, G.A., Sevignani, C., Dumitru, C.D., Hyslop, T., Noch, E., Yendamuri, S., Shimizu, M., Rattan, S., Bullrich, F., Negrini, M., and Croce, C.M. (2004). Human microRNA genes are frequently located at fragile sites and genomic regions involved in cancers. Proc. Natl. Acad. Sci. USA *101*, 2999–3004.

Ceol, C.J., and Horvitz, H.R. (2004). A new class of *C. elegans* synMuv genes implicates a Tip60/NuA4-like HAT complex as a negative regulator of Ras signaling. Dev. Cell *6*, 563–576.

Chang, S., Johnston, R.J., Jr., Frokjaer-Jensen, C., Lockery, S., and Hobert, O. (2004). MicroRNAs act sequentially and asymmetrically to control chemosensory laterality in the nematode. Nature *430*, 785–789.

Chen, C.Z., Li, L., Lodish, H.F., and Bartel, D.P. (2004). MicroRNAs modulate hematopoietic lineage differentiation. Science *303*, 83–86.

Dent, J.A., and Han, M. (1998). Post-embryonic expression pattern of C. elegans *let-60 ras* reporter constructs. Mech. Dev. *72*, 179–182.

Eisenmann, D.M., and Kim, S.K. (1997). Mechanism of activation of the Caenorhabditis elegans *ras* homologue *let-60* by a novel, temperature-sensitive, gain-of-function mutation. Genetics *146*, 553–565.

Gauwerky, C.E., Huebner, K., Isobe, M., Nowell, P.C., and Croce, C.M. (1989). Activation of MYC in a masked t(8;17) translocation results in an aggressive B-cell leukemia. Proc. Natl. Acad. Sci. USA *86*, 8867–8871.

Grosshans, H., Johnson, T., Reinert, K.L., Gerstein, M., and Slack, F.J. (2005). The temporal patterning microRNA let-7 controls several transcription factors during the larval to adult transition in C. elegans. Dev. Cell *8*, 321–330.

Han, M., Aroian, R.V., and Sternberg, P.W. (1990). The *let-60* locus controls the switch between vulval and nonvulval cell fates in Caenorhabditis elegans. Genetics *126*, 899–913.

Han, M., and Sternberg, P.W. (1990). *let-60*, a gene that specifies cell fates during *C. elegans* vulval induction, encodes a *ras* protein. Cell *63*, 921–931.

Hopper, N.A., Lee, J., and Sternberg, P.W. (2000). ARK-1 inhibits EGFR signaling in *C. elegans*. Mol. Cell *6*, 65–75.

Hutvágner, G., Simard, M.J., Mello, C.C., and Zamore, P.D. (2004). Sequence-specific inhibition of small RNA function. PLoS Biol. *2(4)*: e98. DOI: 10.1371/journal.pbio.0020098.

Johnson, L., Mercer, K., Greenbaum, D., Bronson, R.T., Crowley, D., Tuveson, D.A., and Jacks, T. (2001). Somatic activation of the *K-ras* oncogene causes early onset lung cancer in mice. Nature *410*, 1111–1116.

Johnson, S.M., Lin, S.Y., and Slack, F.J. (2003). The time of appearance of the *C. elegans let-7* microRNA is transcriptionally controlled utilizing a temporal regulatory element in its promoter. Dev. Biol. *259*, 364–379.

Johnston, R.J., and Hobert, O. (2003). A microRNA controlling left/right neuronal asymmetry in Caenorhabditis elegans. Nature *426*, 845–849.

Katz, W.S., Hill, R.J., Clandinin, T.R., and Sternberg, P.W. (1995). Different levels of the *C. elegans* growth factor LIN-3 promote distinct vulval precursor fates. Cell *82*, 297–307.

Lagos-Quintana, M., Rauhut, R., Lendeckel, W., and Tuschl, T. (2001). Identification of novel genes coding for small expressed RNAs. Science *294*, 853–858.

Lagos-Quintana, M., Rauhut, R., Yalcin, A., Meyer, J., Lendeckel, W., and Tuschl, T. (2002). Identification of tissue-specific microRNAs from mouse. Curr. Biol. *12*, 735–739.

Lau, N.C., Lim, L.P., Weinstein, E.G., and Bartel, D.P. (2001). An abundant class of tiny RNAs with probable regulatory roles in *Caenorhabditis elegans*. Science *294*, 858–862.

Lee, R.C., and Ambros, V. (2001). An extensive class of small RNAs in *Caenorhabditis elegans*. Science *294*, 862–864.

Lee, R.C., Feinbaum, R.L., and Ambros, V. (1993). The *C. elegans* heterochronic gene *lin-4* encodes small RNAs with antisense complementarity to *lin-14*. Cell *75*, 843–854.

Lee, J., Jongeward, G.D., and Sternberg, P.W. (1994). *unc-101*, a gene required for many aspects of *Caenorhabditis elegans* development and behavior, encodes a clathrin-associated protein. Genes Dev. *8*, 60–73.

Lewis, B.P., Shih, I.H., Jones-Rhoades, M.W., Bartel, D.P., and Burge, C.B. (2003). Prediction of mammalian microRNA targets. Cell *115*, 787–798.

Lim, L.P., Lau, N.C., Weinstein, E.G., Abdelhakim, A., Yekta, S., Rhoades, M.W., Burge, C.B., and Bartel, D.P. (2003). The microRNAs of Caenorhabditis elegans. Genes Dev. *17*, 991–1008.

Lin, S.Y., Johnson, S.M., Abraham, M., Vella, M.C., Pasquinelli, A., Gamberi, C., Gottlieb, E., and Slack, F.J. (2003). The *C. elegans*

*hunchback* homolog, *hbl-1*, controls temporal patterning and is a probable microRNA target. Dev. Cell *4*, 639–650.

Malumbres, M., and Barbacid, M. (2003). RAS oncogenes: the first 30 years. Nat. Rev. Cancer *3*, 459–465.

McKay, I.A., Marshall, C.J., Cales, C., and Hall, A. (1986). Transformation and stimulation of DNA synthesis in NIH-3T3 cells are a titratable function of normal p21N-ras expression. EMBO J. *5*, 2617–2621.

McManus, M.T. (2003). MicroRNAs and cancer. Semin. Cancer Biol. *13*, 253–258.

Meister, G., Landthaler, M., Dorsett, Y., and Tuschl, T. (2004). Sequence-specific inhibition of microRNA- and siRNA-induced RNA silencing. RNA *10*, 544–550.

Michael, M.Z., O'Connor, S.M., van Holst Pellekaan, N.G., Young, G.P., and James, R.J. (2003). Reduced accumulation of specific microRNAs in colorectal neoplasia. Mol. Cancer Res. *1*, 882–891.

Moss, E.G., Lee, R.C., and Ambros, V. (1997). The cold shock domain protein LIN-28 controls developmental timing in *C. elegans* and is regulated by the lin-4 RNA. Cell *88*, 637–646.

Pasquinelli, A., Reinhart, B., Slack, F., Maller, B., and Ruvkun, G. (2000). Conservation across animal phylogeny of the sequence and temporal regulation of the 21 nucleotide C. elegans *let-7* heterochronic regulatory RNA. Nature *408*, 86–89.

Pulciani, S., Santos, E., Long, L.K., Sorrentino, V., and Barbacid, M. (1985). *ras* gene amplification and malignant transformation. Mol. Cell. Biol. *5*, 2836–2841.

Reinhart, B., Slack, F., Basson, M., Pasquinelli, A., Bettinger, J., Rougvie, A., Horvitz, R., and Ruvkun, G. (2000). The 21 nucleotide *let-7* RNA regulates C. elegans developmental timing. Nature *403*, 901–906.

Slack, F.J., Basson, M., Liu, Z., Ambros, V., Horvitz, H.R., and Ruvkun, G. (2000). The *lin-41* RBCC gene acts in the *C. elegans* heterochronic pathway between the *let-7* regulatory RNA and the *lin-29* transcription factor. Mol. Cell *5*, 659–669.

Stein, L.D., Bao, Z., Blasiar, D., Blumenthal, T., Brent, M.R., Chen, N., Chinwalla, A., Clarke, L., Clee, C., Coghlan, A., et al. (2003). The genome sequence of Caenorhabditis briggsae: a platform for comparative genomics. PLoS Biol. *1(2)* e45 DOI: 10.1371/journal.pbio.0000045.

Sternberg, P.W. (1988). Lateral inhibition during vulval induction in Caenorhabditis elegans. Nature *335*, 551–554.

Sulston, J.E., and Horvitz, H.R. (1977). Post-embryonic cell lineages of the nematode, Caenorhabditis elegans. Dev. Biol. *56*, 110–156.

Takamizawa, J., Konishi, H., Yanagisawa, K., Tomida, S., Osada, H., Endoh, H., Harano, T., Yatabe, Y., Nagino, M., Nimura, Y., et al. (2004). Reduced expression of the let-7 microRNAs in human lung cancers in association with shortened postoperative survival. Cancer Res. *64*, 3753–3756.

Tam, W. (2001). Identification and characterization of human *BIC*, a gene on chromosome 21 that encodes a noncoding RNA. Gene *274*, 157–167.

Tam, W., Hughes, S.H., Hayward, W.S., and Besmer, P. (2002). Avian *bic*, a gene isolated from a common retroviral site in avian leukosis virus-induced lymphomas that encodes a noncoding RNA, cooperates with *c-myc* in lymphomagenesis and erythroleukemogenesis. J. Virol. *76*, 4275–4286.

Tan, P.B., Lackner, M.R., and Kim, S.K. (1998). MAP kinase signaling specificity mediated by the LIN-1 Ets/LIN-31 WH transcription factor complex during *C. elegans* vulval induction. Cell *93*, 569–580.

Timmons, L., Court, D.L., and Fire, A. (2001). Ingestion of bacterially expressed dsRNAs can produce specific and potent genetic interference in Caenorhabditis elegans. Gene *263*, 103–112.

Vella, M.C., Choi, E.-Y., Lin, S.Y., Reinert, K., and Slack, F.J. (2004). The C. elegans microRNA *let-7* binds to imperfect *let-7* complementary sites from the *lin-41* 3′UTR. Genes Dev. *18*, 132–137.

Wang, M., and Sternberg, P.W. (2001). Pattern formation during C. elegans vulval induction. Curr. Top. Dev. Biol. *51*, 189–220.

Wightman, B., Ha, I., and Ruvkun, G. (1993). Posttranscriptional regulation of the heterochronic gene *lin-14* by *lin-4* mediates temporal pattern formation in *C. elegans*. Cell *75*, 855–862.

Yoo, A.S., Bais, C., and Greenwald, I. (2004). Crosstalk between the EGFR and LIN-12/Notch pathways in C. elegans vulval development. Science *303*, 663–666.

Yoon, C.H., Lee, J., Jongeward, G.D., and Sternberg, P.W. (1995). Similarity of *sli-1*, a regulator of vulval development in C. elegans, to the mammalian proto-oncogene *c-cbl*. Science *269*, 1102–1105.

**Accession Numbers**

The following sequences were searched for 3′UTR LCSs: *Hs KRAS* (GenBank M54968), *Hs HRAS* (NM176795), *Hs NRAS* (BC005219). NRAS is known to exist as a 2 kb and a 4.3 kb form. BC005219 represents the short form with an 1151 nt polyadenylated 3′UTR. We sequenced two human EST clones (GenBank BU177671 and BG388501) to obtain additional *NRAS* 3′UTR sequence. This revealed that the *NRAS* 3′UTR exists in a 3642 nt polyadenylated 3′UTR version, utilizing an alternative polyadenylation and cleavage site, 2491 nt downstream of the first. This presumably corresponds to the long NRAS form. The sequences were deposited with accession numbers AY941100 and AY941101.